Journal of Algorithms and Computations

journal homepage: http://jac.ut.ac.ir

Sigmoid derivative mapping of full tensor potential field gravity data for edge enhancement

M. Abedi[*1]

[1] Petroleum Engineering and Geophysics Laboratory, School of Mining Engineering, College of Engineering University of Tehran, Iran

ABSTRACT

Airborne gravity gradient surveys yield comprehensive measurements of the Earth's gravity tensor, offering critical insights for geological structural analysis. These data facilitate the delineation of subsurface sources and the spatial extent of structures responsible for gravity anomalies through the integrated interpretation of each tensor component. Given the inherent gradient nature of the acquired data, their combined analysis serves as a robust tool for enhancing structural boundary detection. However, airborne gravity gradient measurements are often significantly contaminated by noise, necessitating the direct utilization of tensor components without further re-derivative to ensure reliable identification of buried targets. In this study, we employ a novel sigmoid derivative function applied to the normalized components of the directional analytical signal of the gradient tensor to improve the resolution of buried target boundaries.

Keywords: Full tensor, Gravity data, Edge enhancement, Sigmoid function, Simulation

ARTICLE INFO

Article history:
Research paper
Received 11 July 2025
Accepted 03 August 2025
Available Online 03 August 2025

AMS subject classification: 68R10.

[†] Corresponding author: M. Abedi, Email: maysamabedi@ut.ac.ir.

1 Introduction

Edge enhancement in potential field data (gravity and magnetic) is a critical technique for interpreting subsurface geological features, such as faults, lithological boundaries, and mineral deposits. These methods enhance discontinuities in geophysical signals, facilitating more precise geological mapping and resource exploration [1,2]. However, the inherent non-uniqueness and noise susceptibility of potential field data pose significant challenges in accurately delineating edges. While first-order derivative-based approaches (e.g., horizontal gradient, tilt angle, and theta map) are commonly employed for edge detection, second-order derivatives have also been utilized [3]. Conventional techniques, such as derivative-based filters, often amplify high-frequency noise, whereas upward continuation tends to attenuate shallow structural features [4]. Recent advancements in edge detection algorithms (e.g., tilt angle, theta map, and normalized total horizontal derivative) and machine learning applications (e.g., convolutional neural networks) seek to optimize the trade-off between sensitivity and robustness [5-7]. Traditional derivative-based methods remain foundational; for instance, the horizontal gradient magnitude (HGM) [8] locates edges by identifying maxima in the first horizontal derivative, while the tilt derivative (TDR) [9] normalizes the vertical gradient by the total horizontal gradient to enhance edge resolution. Nevertheless, these approaches are inherently noise-sensitive and may generate artifacts in low signal-to-noise-ratio (SNR) environments [4].

To overcome these limitations, advanced enhancement techniques have been developed. The analytic signal amplitude method integrates horizontal and vertical derivatives, generating amplitude maxima that coincide with source boundaries [10,11]. Recent innovations include hyperbolic edge detectors, such as the total horizontal derivative of the tilt angle [12] and its normalized variants [5], which exhibit enhanced edge resolution while preserving robustness against noise. These methods exploit higher-order derivatives to sharpen edge delineation and mitigate spurious artifacts of non-geological origin.

Multiscale approaches have emerged to address the inherent depth ambiguity in potential field data. Wavelet transform methods analyze field anomalies at multiple scales, enabling simultaneous detection of both shallow and deep-seated structures [13]. Similarly, Euler deconvolution, when applied with appropriate structural indices, can simultaneously estimate edge locations and source depths [14,15]. These methods have proven particularly valuable in complex geological settings where structures occur at multiple depth levels [16].

The advent of machine learning has opened new frontiers in edge detection. Deep learning frameworks, especially those employing U-Net architectures, have demonstrated exceptional capability in automated edge identification while exhibiting significant noise resilience [17]. These data-driven methods possess the capacity to extract intricate patterns from extensive training datasets, offering potential solutions to certain constraints inherent in conventional physics-based methods. However, their implementation necessitates substantial quantities of high-fidelity training data and often suffers from reduced interpretability compared to traditional approaches. Notwithstanding these technological advancements, several critical challenges persist in edge detection applications: (1) achieving optimal trade-offs between sensitivity to near-surface features and deeper structural resolution, (2) developing noise suppression techniques capable of preserving authentic geological boundaries, and (3) enhancing computational performance to accommodate increasingly large-scale geophysical surveys.

Conventional gravity surveys have traditionally depended on scalar measurements of the vertical gravitational field component [1]. In contrast, modern technological developments, particularly full tensor gravity gradiometry (FTG), now enable multi-component acquisition of the complete gravity gradient tensor, yielding superior resolution and enhanced sensitivity to subsurface density variations. Edge detection techniques are crucial in interpreting potential field data, as they help identify geological boundaries, such as faults, intrusions, and basin margins. However, the application of these techniques to FTG data remains an area of active research due to the increased dimensionality and information content of tensor measurements. The gravity gradient tensor provides additional constraints on subsurface structures, as each component responds differently to lateral density variations. Edge detection methods adapted for FTG data, such as the symmetric eigenvalue analysis [18,19], the modulus of full tensor gravity gradient [20] or the invariants-based approach [21], offer improved localization of geological boundaries compared to conventional scalar-based methods.

Noise in potential field data—whether from instrumentation errors, terrain effects, or cultural interference—significantly degrades the performance of edge detection algorithms, often leading to false anomalies and reduced interpretability. High-frequency noise can artificially enhance gradient-based edge detectors. Conversely, low-frequency noise (e.g., regional trends or platform motion in airborne surveys) may suppress subtle discontinuities, particularly in tensor gravity gradiometry data, where small-amplitude signals are critical. Given the deleterious impact of noise on boundary detection methodologies and the inherent noise susceptibility of airborne gravity gradient tensor measurements, this study employs a novel approach combining normalized directional analytical signal functions with a sigmoid derivative operator. Our methodology directly utilizes the original measured gravity gradient tensor components as inputs to the sigmoid derivative, bypassing conventional approaches that require additional numerical differentiation of input data - a process known to amplify noise artifacts. This integrated framework enables robust boundary detection while maintaining the signal fidelity of the original measurements, thereby mitigating the noise propagation issues inherent in traditional derivative-based edge detection algorithms.

2 Full tensor gravity data

The FTG data acquisition system measures the complete Gravity Gradient Tensor (GGT), delivering a high-resolution characterization of subsurface density variations. In contrast to traditional gravity surveys, which are limited to recording only the vertical component of the gravitational field (G_z), FTG captures all five independent components of the GGT. This comprehensive measurement enhances structural resolution and mitigates interpretational ambiguities in geophysical inversion [22]. Following Pedersen and Rasmussen (1990), we review key properties of the GGT. The gravitational potential U generated by an anomalous density distribution ρ within a volume V is expressed as

$$U(\boldsymbol{r}) = -\gamma \int_V \frac{\rho(\boldsymbol{r}')}{|\boldsymbol{r}-\boldsymbol{r}'|} dv',$$

Here, $\boldsymbol{r}$ and $\boldsymbol{r}'$ represent the observation and integration points, respectively, and γ denotes the universal gravitational constant. The gravitational gradient tensor at location $\boldsymbol{r}$, generated by a density distribution $\rho(\boldsymbol{r}')$, is given by [23]:

$$\Gamma_{ij}(\boldsymbol{r}) = -\gamma \int_V \rho(\boldsymbol{r}') \frac{\partial^2}{\partial x_i \partial x_j} \frac{1}{|\boldsymbol{r}-\boldsymbol{r}'|} dv',$$

where x_i or x_j correspond to the three orthogonal coordinate axes. Consequently, the gravity gradient tensor $\mathbf{\Gamma}$ expressed as:

$$\mathbf{\Gamma} = \begin{bmatrix} \frac{\partial^2 U}{\partial x^2} & \frac{\partial^2 U}{\partial x \partial y} & \frac{\partial^2 U}{\partial x \partial z} \\ \frac{\partial^2 U}{\partial y \partial x} & \frac{\partial^2 U}{\partial y^2} & \frac{\partial^2 U}{\partial y \partial z} \\ \frac{\partial^2 U}{\partial z \partial x} & \frac{\partial^2 U}{\partial z \partial y} & \frac{\partial^2 U}{\partial z^2} \end{bmatrix}$$

The GGT can also be written as

$$\mathbf{\Gamma} = \begin{bmatrix} \frac{\partial}{\partial_x} \\ \frac{\partial}{\partial_y} \\ \frac{\partial}{\partial_z} \end{bmatrix} \begin{bmatrix} G_x & G_y & G_z \end{bmatrix} = \begin{bmatrix} \frac{\partial G_x}{\partial x} & \frac{\partial G_x}{\partial y} & \frac{\partial G_x}{\partial z} \\ \frac{\partial G_y}{\partial x} & \frac{\partial G_y}{\partial y} & \frac{\partial G_y}{\partial z} \\ \frac{\partial G_z}{\partial x} & \frac{\partial G_z}{\partial y} & \frac{\partial G_z}{\partial z} \end{bmatrix} = \begin{bmatrix} G_{xx} & G_{xy} & G_{xz} \\ G_{yx} & G_{yy} & G_{yz} \\ G_{zx} & G_{zy} & G_{zz} \end{bmatrix}$$

where the gravitational field vector $\boldsymbol{G} = (G_{x,} G_{y,} G_z)$ represents the three components of the gravity field [21]. In source-free regions (free space), the gravitational potential U satisfies Laplace's equation [1],

$$div\ \boldsymbol{G} = \nabla . \mathbf{G} = \nabla^2 U(\boldsymbol{r}) = 0$$

Consequently, the trace of the tensor $Trace(\mathbf{\Gamma}) = G_{xx} + G_{yy} + G_{zz} = 0$. In addition, the curl of $\boldsymbol{G}$ field is zero

$$curl\ \boldsymbol{G} = \nabla \times \mathbf{G} = \begin{vmatrix} i & j & k \\ \frac{\partial}{\partial x} & \frac{\partial}{\partial x} & \frac{\partial}{\partial x} \\ G_x & G_y & G_z \end{vmatrix} = 0$$

According to above Equation, the gravity gradient tensor $\mathbf{\Gamma}$ is symmetric,

$$\begin{cases} \frac{\partial G_x}{\partial y} = \frac{\partial G_y}{\partial x} \\ \frac{\partial G_x}{\partial z} = \frac{\partial G_z}{\partial x} \\ \frac{\partial G_y}{\partial z} = \frac{\partial G_z}{\partial y} \end{cases}$$

According to the above formulas, $\mathbf{\Gamma}$ can be rewritten as,

$$\mathbf{\Gamma} = \begin{bmatrix} G_{xx} & G_{xy} & G_{xz} \\ G_{xy} & G_{yy} & G_{yz} \\ G_{xz} & G_{yz} & -(G_{xx} + G_{yy}) \end{bmatrix}$$

Consequently, the preceding analysis demonstrates that the GGT can be fully characterized through measurement of just five independent components, as dictated by its inherent symmetry properties.

3 Sigmoid derivative mapping

Beiki (2010) established the mathematical formulation for the directional analytical signal amplitude as follows [24]:

$$A_x = \sqrt{{G_{xx}}^2 + {G_{xy}}^2 + {G_{xz}}^2}$$

$$A_y = \sqrt{{G_{yx}}^2 + {G_{yy}}^2 + {G_{yz}}^2}$$

$$A_z = \sqrt{{G_{zx}}^2 + {G_{zy}}^2 + {G_{zz}}^2}$$

The subscripts x, y, and z correspond to the three orthogonal spatial directions. Maxima in A_x delineate north-south oriented edges, while maxima in A_y identify east-west oriented boundaries. The vertical component A_z represents the conventional analytical signal as defined by [25]. To facilitate comparison between directional components, we employ a normalized ratio function R expressed as:

$$R = \frac{A_z}{\sqrt{{A_x}^2 + {A_y}^2}}$$

The sigmoid function (also called the logistic function) is an *S*-shaped, monotonically increasing function that maps real numbers to an (0,1) interval [26]. It is defined as:

$$\sigma(x, P) = \frac{1}{1 + e^{-x/P}}$$

and its derivative equals to,

$$\sigma'(x, P) = \frac{1}{P}\sigma(x, P)[1 - \sigma(x, P)]$$

Figure 1 illustrates the sigmoid function and its corresponding derivative across six distinct parameter values (P). Subsequent analysis will employ this function to characterize the spatial variation of parameter R.

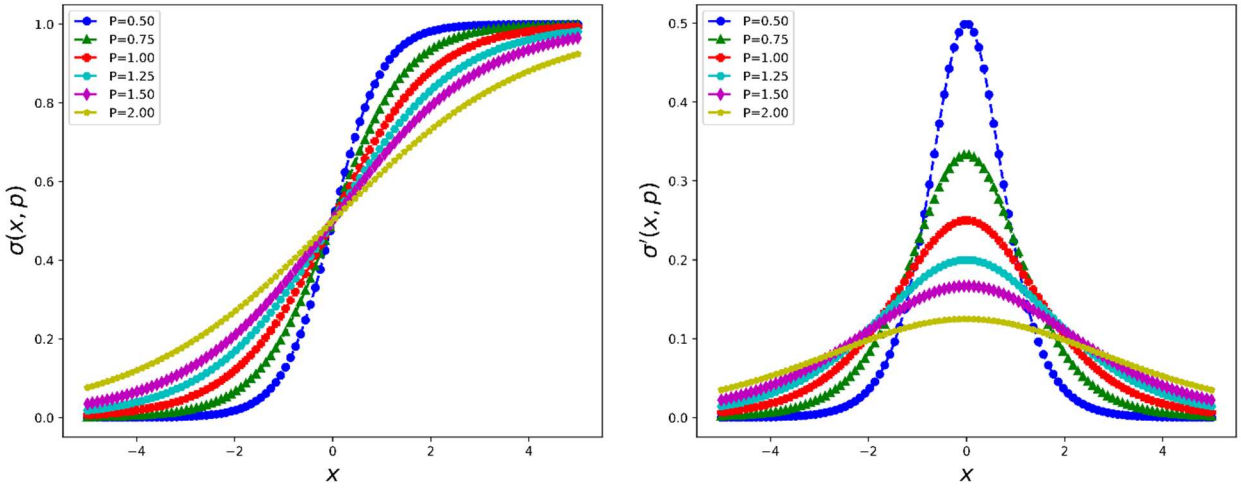

Figure 1: Sigmoid function and its derivative for different value of P

4 Numerical experiment

To assess the effectiveness of the proposed boundary detection algorithm, a comprehensive numerical simulation was conducted utilizing gravity gradient tensor data. This simulation was set within a defined area measuring 1000 meters in both length and width, where three distinct geological structures were modeled. These structures were assigned density contrasts of 0.8, 1, and 0.9 gr/cm^3, respectively, in relation to the surrounding medium, arranged sequentially from left to right. The depths of these structures were specified at 50, 150, and 100 meters. An open source framework "SimPEG" was used to simulate data [27]. The simulated geological configuration is illustrated in two distinct sections—horizontal and depth—depicted in Figure 2. To enhance realism, the generated data incorporated noise, characterized by a standard deviation equivalent to one percent of the maximum data value, with a mean of zero. The three-component gravity field data are illustrated in Figure 3, with Figure 4 displaying the complete gravity gradient tensor representation. Accurate delineation of the three synthetic source bodies requires implementation of advanced boundary detection methodologies, highlighting the critical role of novel analytical approaches in modern geophysical interpretation.

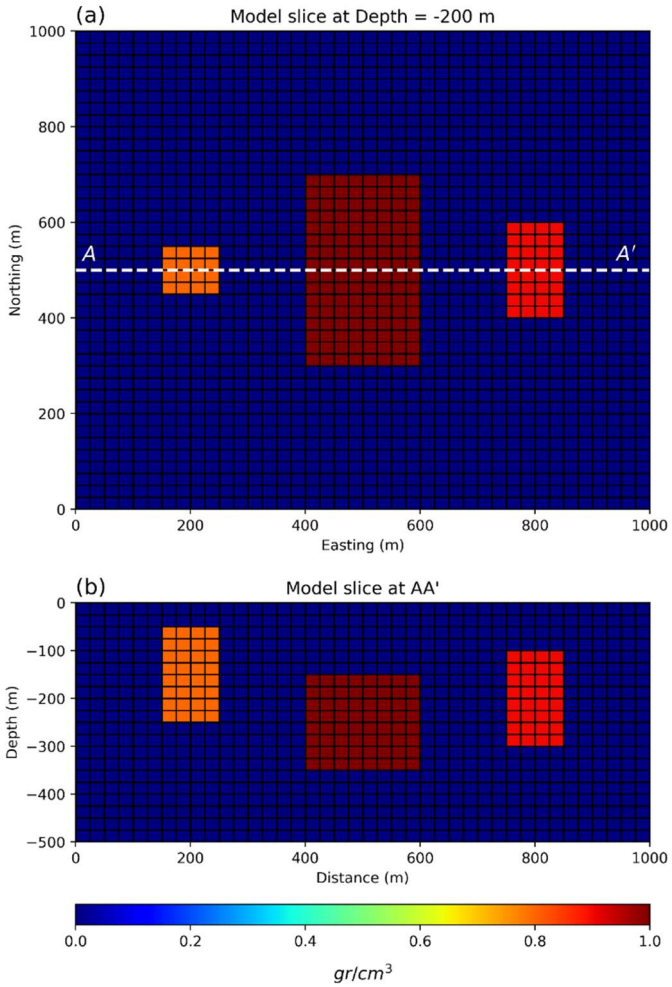

Figure 2: The visualization density contrast of synthetic multi source model, (a) plan view at depth 200 m, and (b) cross section along profile AA'

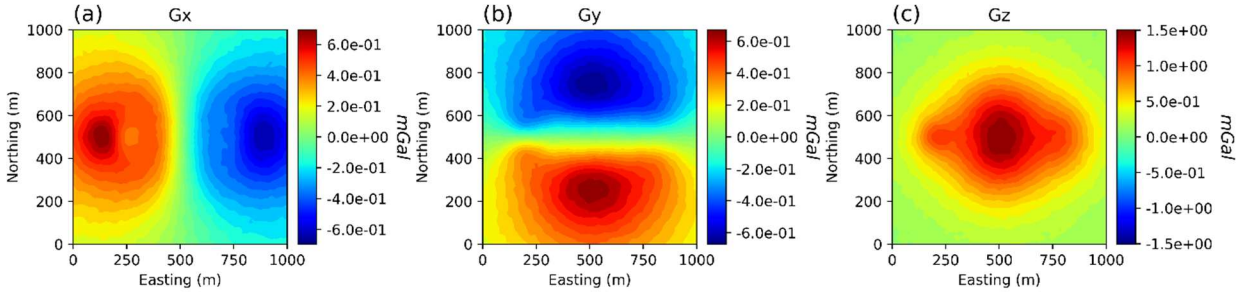

Figure 3: Three directional components of gravity data for synthetic multi source model. Data have been corrupted with 1% random Gaussian noise

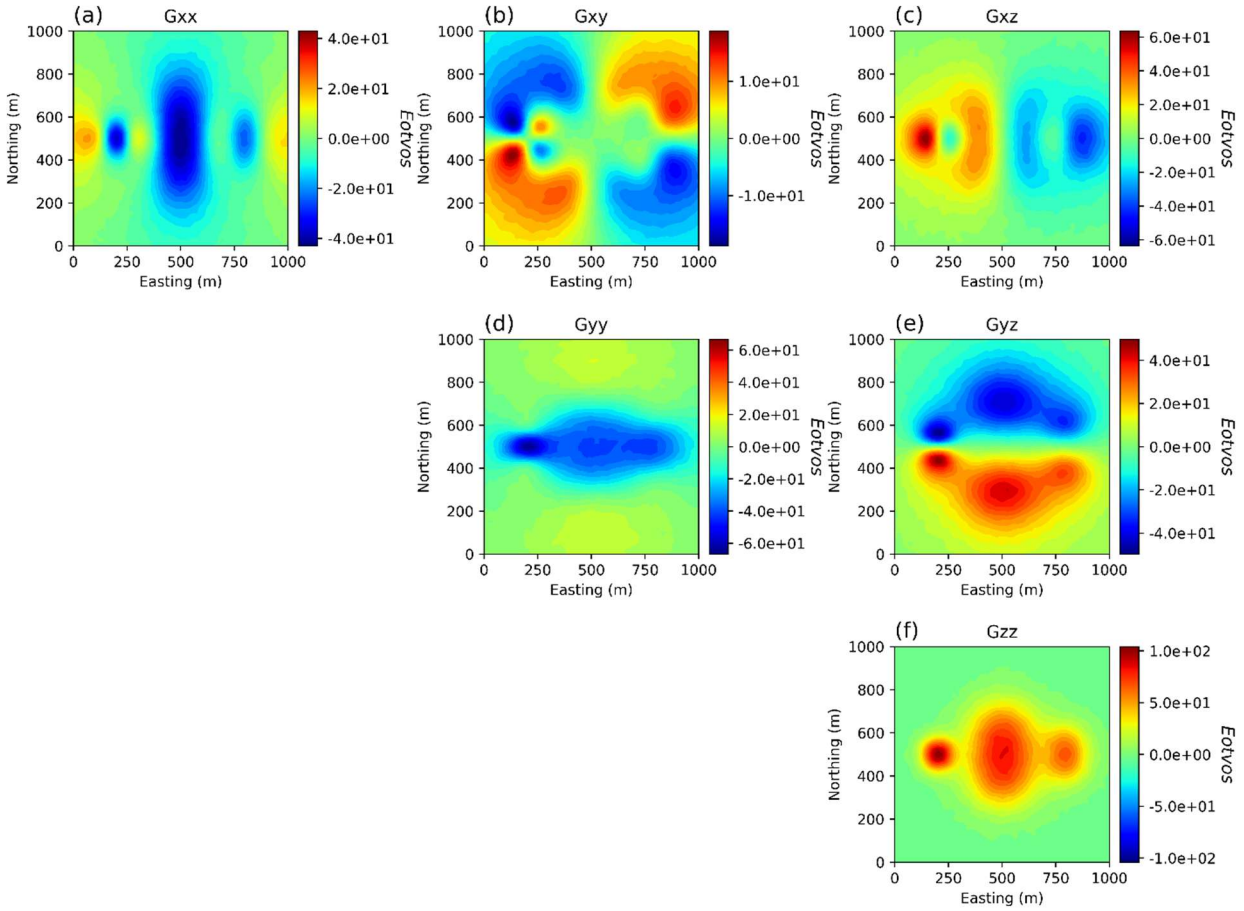

Figure 4: Full tensor gradients of gravity data for synthetic multi source model. Data have been corrupted with 1% random Gaussian noise

Following the computation of the normalized R value derived from the directional analytical signals, the sigmoid derivative function was evaluated across six distinct values of P, ranging from 0.5 to 2. The resulting data was visually represented in Figure 5, specifically in the second and third rows. Additionally, this analysis was extended along the AA' profile illustrated in Figure 2, with the outcomes for varying P values displayed in the first row of Figure 5. Notably, as the value of P increases, the delineation of the three hypothesized targets becomes increasingly distinct, showcasing a remarkable separation between their boundaries. These delineations exhibit a strong correlation with the initially presented boundaries, which had proven challenging to extract from the gravity gradient tensor data. Furthermore, it is significant to highlight that along the AA' profile, the minimum points of the curves effectively indicate the centers of the three targets, reinforcing the accuracy of the analysis.

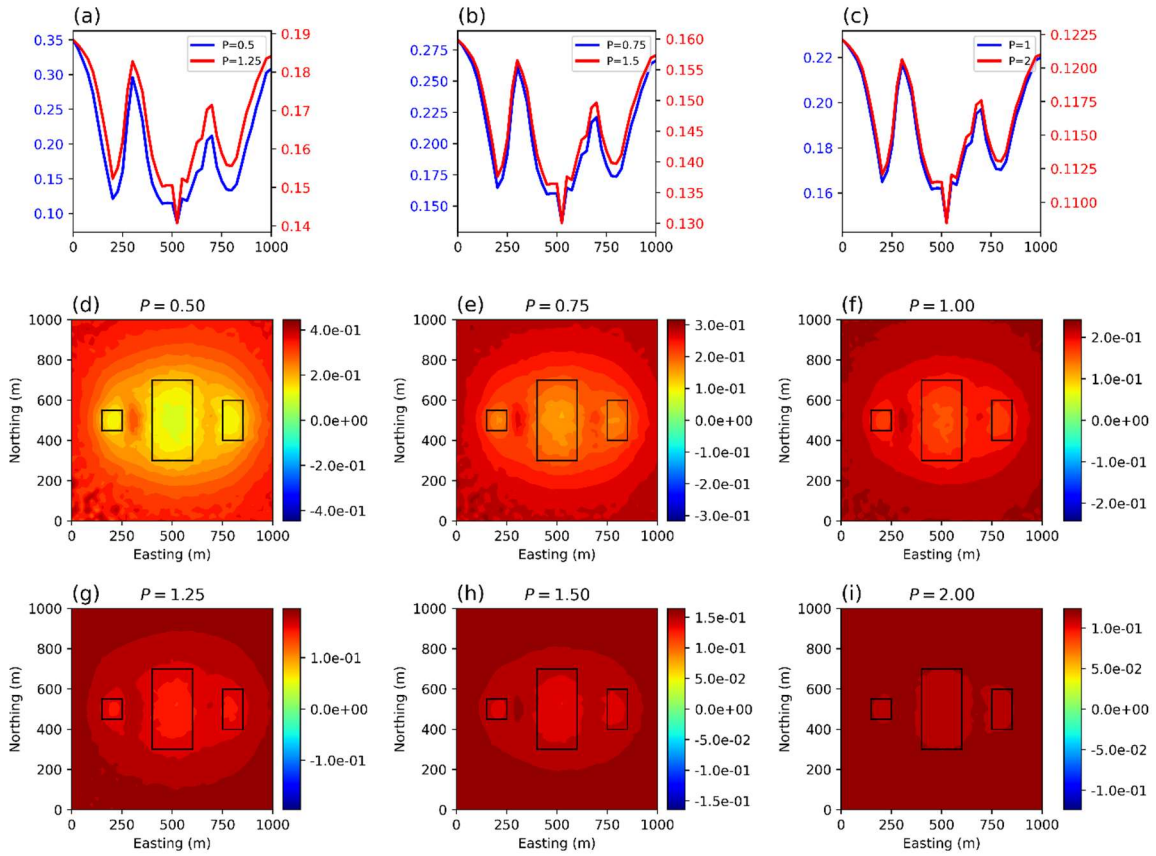

Figure 5: Sigmoid derivative mapping of full tensor gravity data for synthetic multi source model. The first row is derivative plot along profile AA' for different value of *P*. The second and third rows are derivative plots for the whole area for different value of *P*

5 Conclusions

A principal challenge in subsurface boundary detection using gravity anomalies stems from the inherent noise contamination in field measurements. The efficacy of directional derivative-based methods deteriorates significantly with increasing noise-to-signal ratios, a phenomenon particularly acute in airborne gravity gradient tensor surveys due to their characteristically elevated noise levels. To overcome these limitations, our study implements a two-stage analytical framework. First, we generate a normalized directional analytical signal map directly from the acquired measurements. Subsequently, we apply a sigmoid derivative operator that successfully enhances the boundaries of synthetic targets, demonstrating significant improvements in both edge resolution and positional accuracy..

Acknowledgments

We extend our heartfelt gratitude to the Faculty of Mining Engineering at the University of Tehran for their invaluable support in the execution of this research.

References

[1] R.J. Blakely, *Potential Theory in Gravity and Magnetic Applications*. Cambridge University Press, 464 P, 1996.

[2] M.N. Nabighian, V.J.S. Grauch, R.O. Hansen, T.R. LaFehr, Y. Li, J.W. Peirce, J.D. Phillips, and M.E. Ruder, *The historical development of the magnetic method in exploration. Geophysics*, 70(6): 1ND-Z113, 2005.

[3] L.T. Pham, R.S. Smith, S.P. Oliveira, and V.T. Jorge, *Enhancing magnetic source edges using the tilt angle of the analytic-signal amplitudes of the horizontal gradient*. Geophysical Prospecting, 72(8): 3026-3037, 2023.

[4] G.R.J. Cooper, and D.R. Cowan, *Enhancing potential field data using filters based on the local phase*. Computers & Geosciences, 32(10): 1585-1591, 2006.

[5] G. Ma, and L. Li, *Edge detection in potential fields with the normalized total horizontal derivative*. Computers & Geosciences, 41: 83-87, 2012.

[6] L.T. Pham, E. Oksum, D.V. Le, F.J.F. Ferreira, and S.T. Le, *Edge detection of potential field sources using the softsign function*. Geocarto International, 37(14): 4255-4268, 2021.

[7] Z. ZhiHou, Y. Yu, S. ZeYu, W. Hu, Q. ZhongKun, W. ShengRen, Q. LiMao, D. ShiHui, L. Feng, and L. WeiXin, *Deep learning for potential field edge detection*. Chinese Journal of Geophysics (in Chinese), 65(5): 1785-1801, 2022.

[8] L. Cordell, and V.J.S. Grauch, *Mapping Basement Magnetization Zones from Aeromagnetic Data in the San Juan Basin, New Mexico*. General Series, 181-197, 1985.

[9] H.G. Miller, and V. Singh, *Potential field tilt - a new concept for location of potential field sources*. Journal of Applied Geophysics, 32 (2-3): 213-217, 1994.

[10] M.N. Nabighian, *The analytic signal of two dimensional magnetic bodies with polygonal cross-section: Its properties and use of automated anomaly interpretation*. Geophysics, 37: 507–517, 1972.

[11] W.R. Roest, J. Verhoef, and M. Pilkington, *Magnetic interpretation using the 3-D analytic signal*. Geophysics, 57(1): 116-125, 1992.

[12] F.J.F. Ferreira, J. de Souza, A.B.S. Bongiolo, and L.G. de Castro, *Enhancement of the total horizontal gradient of magnetic anomalies using the tilt angle*. Geophysics, 78(3): J33-J41, 2013.

[13] P. Hornby, F. Boschetti, and F.G. Horowitz, *Analysis of potential field data in the wavelet domain*. Geophysical Journal International, 137(1): 175-196, 1999.

[14] A.B. Reid, J.M. Allsop, H. Granser, A.J. Millett, and I.W. Somerton, *Magnetic interpretation in three dimensions using Euler deconvolution*. Geophysics, 55(1): 80-91, 1990.

[15] D.T. Thompson, *EULDPH: A new technique for making computer-assisted depth estimates from magnetic data*. Geophysics, 47(1): 31-37, 1982.

[16] A. Salem, S. Williams, J.D. Fairhead, R. Smith, and D. Ravat, *Interpretation of magnetic data using tilt-angle derivatives*. Geophysics, 73(1): L1-L10, 2008.

[17] X. Wu, L.Liang, Y. Shi, and S. Fomel, *FaultSeg3D: Using synthetic datasets to train an end-to-end convolutional neural network for 3D seismic fault segmentation*. Geophysics, 84(3): IM35-IM45, 2019.

[18] L.B. Pedersen, and T.M. Rasmussen, *The gradient tensor of potential field anomalies: Some implications on data collection and data processing of maps*. Geophysics, 55(12): 1558-1566, 1990.

[19] Y. Yuan, X. Zhang, W. Zhou, G. Wu, and W. Luo, *Application of the normalized largest eigenvalue of structure tensor in the interpretation of potential field tensor data*. Planets and Space, 72: 143, 2020.

[20] H. Wu, L. Li, C. Xing, and S. Zhang*, A new method of edge detection based on the total horizontal derivative and the modulus of full tensor gravity gradient*. Journal of Applied Geophysics, 139: 239-245, 2017.

[21] M. Beiki, and L.B. Pedersen, *Eigenvector analysis of gravity gradient tensor to locate geologic bodies*. Geophysics, 75(6): I37-I49, 2010.

[22] M.S. Zhdanov, *Inverse Theory and Applications in Geophysics*. 2nd ed. Amsterdam: Elsevier, 685 p, 2015.

[23] D. Nagy, G. Papp, and J. Benedek, *The gravitational potential and its derivatives for the prism*. Journal of Geodesy, 74 (7-8): 552-560, 2000.

[24] Beiki, M., *Analytical signals of gravity gradient tensor and their application to estimate source location*. Geophysics, 75(6): I59–I74, 2010.

[25] Y. Yuan, and Q. Yu, *Edge Detection in Potential-Field Gradient Tensor Data by Use of Improved Horizontal Analytical Signal Methods*. Pure and Applied Geophysics, 172(2): 461-472, 2014.

[26] C.M. Bishop, *Pattern Recognition and Machine Learning*. New York: Springer, 73 P, 2006.

[27] R. Cockett, S. Kang, L.J. Heagy, A. Pidlisecky, and D.W. Oldenburg, *SimPEG: An Open Source Framework for Simulation and Gradient Based Parameter Estimation in Geophysical Applications*. Computers & Geosciences, 85: 142-154, 2015.